Journal of Computers Vol. 31 No. 2, 2020, pp. 298-311
doi:10.3966/199115992020043102025

Abdominal Needle Assisted Robotic Arm Motion Control and Trajectory Planning

Ying-Gang Xie[1*], Guang-Jun Liu[2], Jiang-Yu Lan[1], Bo-Bin Gao[1]

[1] Beijing Information Science and Technology University, Beijing 100101, China
xieyinggang@bistu.edu.cn, ljy960716@163.com, gaobobinbin@126.com

[2] Department of Aerospace Engineering, Ryerson University, Toronto, ON M5B 2K3, Canada
gjliu@ryerson.ca

Received 20 January 2020; Revised 20 February 2020; Accepted 30 March 2020

Abstract. Abdominal massage is a new maintenance method based on the theory of abdominal acupuncture. This article designs and develops an acupuncture-assisted robotic arm that can perform acupoint measurement and acupoint click massage. The abdominal needle auxiliary robotic arm uses a single-chip microcomputer control board to control the three-axis large stepping motor arm. The laser ranging sensor is used at the end to detect the exact distance between the robot arm and the human abdomen. Based on machine vision to realize the judgment of reference points, the infrared auxiliary marker is used. In this paper, according to the calculated coordinates of acupoints, the arc-trajectory planning algorithm is realized based on the equal-division interpolation of space arc, the motion planning of abdominal needle massage robot manipulator and the coordination of triaxial motor are completed, and the motion trajectory of abdominal cartesian coordinates is simulated. According to the axial variables, the system solves the attitude matrix at the end to achieve the acupoint marking, which can meet the real-time and accuracy of the triaxial abdominal needle massage robot motion planning under the feedback of external sensor information.

Keywords: acupuncture assisted robot, kinematic equation, manipulator motion control, trajectory planning

1 Introduction

Acupuncture has a history of more than 2,000 years in China and is a very important part of the medical and health field in China. Abdominal acupuncture therapy is a representative new acupuncture method after more than 20 years of repeated clinical practice, which inherits the research results of traditional Chinese medicine and modern medicine on meridians [1-2]. With the rapid development of robot technology, it is possible to develop intelligent acupuncture robot, and many structures are studied around its related core technology [3]. Now robots have been used in every part of our lives [4-5]. Other applications of service robots and light robotic arms have been widely used in medical treatment, rescue and other industries [6]. It has been widely used in defense, industrial and medical fields, using robotic arms to transfer and locate objects [7-8].

Fudan University in Shanghai has carried out the project of an independent interactive intelligent TCM service robot and its system platform. Guided by the basic theory of TCM, it has combined the objective research of TCM with an intelligent robot and artificial intelligence technology to design and develop TCM health service robot terminal and intelligent cloud platform [9]. The arm rehabilitation robot has a mit-manus arm assisted rehabilitation system developed by the Massachusetts Institute of technology in the United States [10]. The robot system for the rehabilitation of paralyzed patients mainly realizes muscle training and strengthening by assisting limb movement. Tolerance, joint flexibility and motor

* Corresponding Author

coordination [11]. The Motion Maker, a rehabilitation robot developed by Swortec SA, can control rehabilitation training based on real-time sensor information and cooperate with electrical stimulation to meet treatment needs [12]. Clinical trials show that the system works well. Harbin engineering university lowers limb rehabilitation robot, arm rehabilitation robot and other systems [13]. The institute of automation of the Chinese academy of sciences has developed a lower limb rehabilitation training robot with EMG signal acquisition and functional electrical stimulation [14]. Novatos et al. [15] by Open CV to polar binocular image correction and stereo matching, get parallax three-dimensional coordinates of the diagram and the point, and the acupuncture will arm robot coordinate transformation relationship and homogeneous transformation matrix coordinates the coordinates can be converted into acupuncture the coordinates of the robot coordinate system, as for the acupuncture operation of the robot positioning.

Acubots digital meridians acupuncture robot team of Nanjing University of Chinese medicine has completed the design of the third generation acupuncture robot products [16]. Based on the cooperative project of abdominal acupuncture research institute, this paper takes the modernization of acupuncture as the research goal, and based on the basic requirements of abdominal acupuncture assisted acupoint marking, develops the abdominal acupuncture assisted mechanical arm, which can help doctors measure and mark acupoints, and further realize the massage based on abdominal acupuncture points. Considering the abdominal needle institute cooperation projects for abdominal needle auxiliary robots cost limit and the requirements of the application environment, this article abdominal needle helpers to triaxial mechanical arm as the basic architecture, at the same time as the basis of acupuncture points based on machine vision calibration positioning method, and based on binocular vision measurement basis points with the length of the mark point area. The emphasis of this paper is on the robot arm control assisted by abdominal needles. For the machine vision and binocular vision of this study, it is not stated as the main point of this paper. Based on the kinematic solution and inverse kinematic equation of the arm, the motion control and trajectory planning of the arm assisted by abdominal acupuncture are realized in this paper. The second chapter reviews the research status of robot arm motion control and trajectory planning. The third part introduces the structure of the robot arm and the frame of the robot arm system assisted by the abdominal needle. The fourth part discusses the arc trajectory planning algorithm based on space arc bisector interpolation. The fifth part introduces the algorithm of abdominal acupoint marking. Section 6 summarizes the paper and Outlines future research trends.

2 Related Work

In terms of solving kinematics of manipulators, the methods to solve the inverse kinematics problem can be divided into the analytical methods and numerical methods. This analysis method has high computational accuracy and efficiency, but it can only be used for certain manipulators and lacks universality [17-18]. Numerical methods require relatively high computer hardware, lack real-time performance, and are difficult to apply online. Jiang li, wait. [19] cuckoo search (CS) was first combined with imperialism. Compared with other intelligent algorithms, this algorithm has higher accuracy in solving robot inverse kinematics. Bayati et al. [20] analyzed the influence of different PSO algorithms on inverse kinematics. Rokbani et al. [21] compared the precision of gravity search algorithm, genetic algorithm, quantum particle swarm optimization algorithm, harmony search algorithm, and particle swarm optimization algorithm to calculate the inverse kinematics of 4-degree-of-freedom robot. D. cloud, etc. [22] based on the adaptive particle swarm optimization algorithm, a mathematical model for solving the inverse kinematics of the multi-degree-of-freedom tandem manipulator is established. Y.-Z. Wang, etc. [23] it was found that the multi-objective particle swarm optimization algorithm solved the inverse kinematics problem of the robot more flexibly. In [24], when calculating the inverse kinematics of a 7-degree-of-freedom manipulator, the position error of the three axes is used as the fitness function of the particle swarm optimization algorithm. [25-26] combining genetic algorithm and particle swarm optimization algorithm, inverse kinematics of multiple end-effectors can be calculated simultaneously. The above intelligent algorithm greatly improves the efficiency of robot inverse kinematics, but the real-time performance of numerical solutions is not significantly improved [27].

In practical application, trajectory planning needs to consider efficiency, energy consumption, stability, and other factors, and optimize for each factor [28-30]. The purpose of the time-optimal trajectory is to improve the working efficiency of the robot and complete the same trajectory as much as possible at the same time. F.-J. Yin, et al. [31] used cubic spline interpolation for trajectory planning, so as to make the

curve of joint angular velocity and angular acceleration smooth and continuous, optimized the trajectory of motion for the shortest time through the adaptive genetic algorithm, and solved the kinematic constraint problem by penalty function. On the basis of the 5-7-5 polynomial interpolation method, H. Chen, et al. [32] took the motion Angle, motion speed and motion acceleration as constraints and adopted the compound shape method for optimization to achieve time optimization. On the one hand, the energy optimal trajectory planning tries to find the smoothest trajectory to reduce the energy loss between the joints, on the other hand, it also tries to optimize the energy distribution through optimizing the whole dynamic system. Gregory, etc. [33] based on b-spline curve interpolation, advances the concept of a "full constraints", to limit velocity and acceleration in the kinematics, dynamics in the joints to limit rotational speed and torque, after comprehensive consideration of various constraints, the change of the energy function greatly narrowed down, thus can more easily find out the optimal energy trajectory, but this method to a certain extent, restrict the performance of the robot. J.-H. Lu, [34] put forward a kind of mechanical arm, such as the optimal time - impact trajectory planning method, using five non-uniform b-spline function interpolation curve in the joint space construction, use of various order B spline curve control points instead of the mechanical arm motion constraints, using the NSGA - II (Non - dominated Sorting based Algorithm II) optimize the objective function. Y. Yu [35] for both robots such as the efficiency and service life, considering the non-uniform b-spline huge amount of calculation and adopted a five uniform b-spline interpolation method on time within the node interpolation in joint space, the algorithm for the hybrid genetic algorithm, first using the optimal time to plan the time-optimal trajectory is obtained and the minimum task time, and in the smallest task time impact adaptive genetic algorithm to search the optimal trajectory.

In this paper, a circular arc trajectory planning algorithm is implemented based on the bisector interpolation of the space arc, which can meet the real-time and accuracy of the motion planning of the three-axis abdominal massage robot with external sensor information feedback.

3 Hardware Design and Implementation

3.1 Design and Implementation of Abdominal Needle Assisted Positioning Device

This topic is based on the robot arm abdominal needle acupuncture point marking device design, emphatically the tested micro miniature mechanical arm range (maximum reach 40 cm) cannot reach all points of the abdomen, in order to satisfy the design of this topic, this topic was designed and implemented the small abdominal needle auxiliary mechanical arm, the largest wingspan 80 cm can meet, abdominal needle acupuncture point location marking requirements.

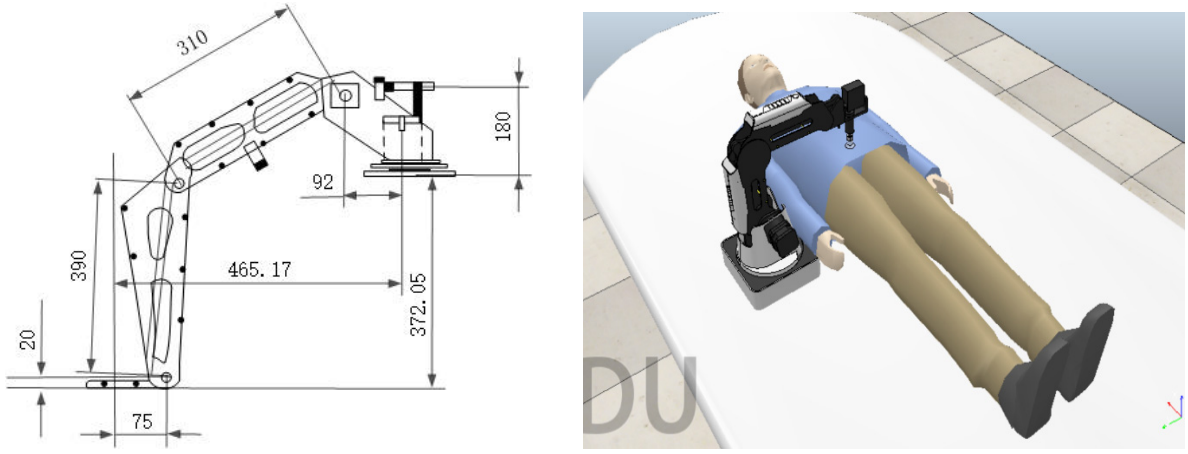

Fig. 1. Organization diagram of abdominal needle assisted positioning device

3.2 Control Principle of Abdominal Needle Auxiliary Positioning Device

Controlling the ventral needle auxiliary positioning device is to control the operation of the stepper motor through the corresponding driver of the stepper motor to achieve the control of the mechanical arm.

Stepper motor is essentially an electromagnetic device with discrete motion, which can realize high precision positioning control. The working principle of the stepper motor is to convert the pulse signal into corresponding angular displacement and adjust the speed and Angle of motor rotation by changing the frequency of the pulse signal.

4 Kinematics Analysis of Abdominal Needle Assisted Positioning Device

4.1 Forward Kinematics Analysis of the Robot Arm

According to the structure of the mechanical arm, when control three direction of motor rotating mechanical arm three-axis trajectory for arc coordinate system, and in the abdomen needle acupuncture point measurement, the acupuncture point calculation process for the rectangular coordinate system, so need to design mechanical arm three-axis coordinated motion to simulate the motion planning of the rectangular coordinate system to ensure that the mechanical arm can be according to the calculation of point coordinates, accurate control of motor move, make the end reaches the specified point position, realize the function of the tag.

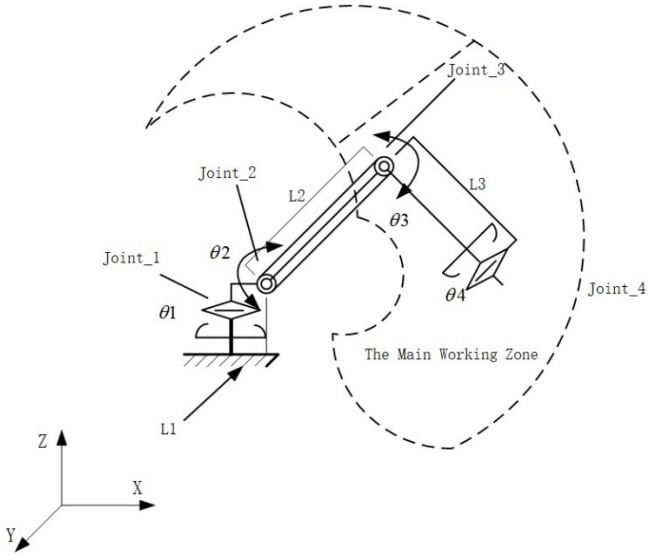

Fig. 2. Robot arm arc coordinate

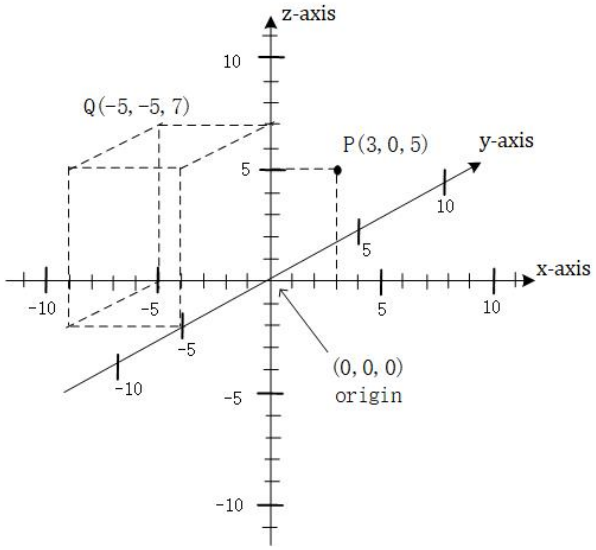

Fig. 3. Corresponding Cartesian coordinate system

$$A_i = Rot(Z,\theta_i)Trans(\alpha_i,0,ld_i)Trans(a_{n+1},0,0)Rot(X,\alpha_i) \tag{1}$$

$$= \begin{bmatrix} \cos\theta_i & -\sin\theta_i & 0 & a_{i-1} \\ \sin\theta_i\cos\alpha_{i-1} & \cos\theta_i\cos\alpha_{i-1} & -\sin\alpha_{i-1} & -\sin\alpha_{i-1}d_i \\ \sin\theta_i\sin\alpha_{i-1} & \cos\theta_i\sin\alpha_{i-1} & -\cos\alpha_{i-1} & \cos\alpha_{i-1}d_i \\ 0 & 0 & 0 & 1 \end{bmatrix} \tag{2}$$

Because the manipulator is a rotary joint. For the manipulator used in this paper, there are five next transformation matrices. The end-chain coordinate system is a homogeneous transformation matrix relative to the base coordinate system [36].

$${}^0_5T = A_1A_2A_3A_4A_5 = \begin{bmatrix} r_{11} & r_{12} & r_{13} & p_x \\ r_{21} & r_{22} & r_{23} & p_y \\ r_{31} & r_{32} & r_{33} & p_z \\ 0 & 0 & 0 & 1 \end{bmatrix} \tag{3}$$

The above robotic arm motion algorithm clearly reflects the equal amount relationship between variables and terminal pose. The joint variable of the five matrices is $q=[\theta_1,\theta_2,\theta_3,\theta_4,\theta_5]^T$. According to the description of rigid body attitude [37], it can be known that r_{11}, r_{12}, r_{13}, r_{21}, r_{22}, r_{23}, r_{31}, r_{32}, r_{33} are respectively the direction cosines of the coordinate axes (X, Y, Z) of the three-dimensional coordinate system of the end of the robot arm and the coordinate system of the bottom of the robot arm, and p_x, p_y, p_z is the three-dimensional coordinate system of the end of the robot arm and the coordinate system of the base of the robot arm.

The essence of solving kinematics of the manipulator is to solve the pose matrix of the end of the manipulator with known axial variables [38]. That is, the joint variable $q=[\theta_1,\theta_2,\theta_3,\theta_4,\theta_5]^T$ is known, and the values of each element of the above equation are solved. The homogeneous transformation matrix of the five joints of the robotic arm in the above equation is substituted into, that is, the values of each element in ${}^0_5T$ are calculated as:

$${}^0_5T = \begin{bmatrix} r_{11} & r_{12} & r_{13} & p_x \\ r_{21} & r_{22} & r_{23} & p_y \\ r_{31} & r_{32} & r_{33} & p_z \\ 0 & 0 & 0 & 1 \end{bmatrix} \tag{4}$$

$$\begin{aligned} r_{11} &= c_1c_{234}c_5 + s_1s_5 \\ r_{12} &= -c_1c_{234}s_5 + s_1c_5 \\ r_{13} &= c_1c_{23}s_4 + c_1s_{23}c_4 \end{aligned} \tag{5}$$

$$\begin{aligned} r_{21} &= s_1c_{234}c_5 - c_1s_5 \\ r_{22} &= -s_1c_{234}s_5 - c_1c_5 \\ r_{23} &= s_1c_{23}s_4 + s_1s_{23}c_4 \end{aligned} \tag{6}$$

$$\begin{aligned} r_{31} &= s_{234}c_5 \\ r_{32} &= -s_{234}s_5 \\ r_{11} &= -c_{234} \end{aligned} \tag{7}$$

$$\begin{aligned} p_x &= c_1c_{23}a_3 + c_1c_2a_2 + s_1ld_2 + c_1a_1 \\ p_y &= s_1c_{23}a_3 + s_1c_2a_2 - c_1ld_2 + s_1a_1 \\ p_z &= s_{23}a_3 + s_2a_2 + ld_1 \end{aligned} \tag{8}$$

Where $c_1 = \cos\theta_1$, $s_1 = \sin\theta_1$, $c_{234} = \cos(\theta_2 + \theta_3 + \theta_4)$, $s_{234} = \sin(\theta_2 + \theta_3 + \theta_4)$

4.2 Trajectory Planning and Simulation of Manipulator Based on Space Arc Interpolation

Calculate the predetermined trajectory curve according to demand. In trajectory planning, we can plan according to kinematics and dynamics [39].

In Cartesian trajectory planning, a new rectangular coordinate system is established on the arc plane, and the value of each interpolation point in the new coordinate system is calculated. Let the end of the robot arm pass through P_2 from the starting position P_1 to the end point P_3. If three points are not collinear, an arc is determined at three points. There must be an arc path planning algorithm that goes through three points. These values are then returned to the original coordinate system to compute the values of the interpolation points in the original coordinate system. And then return those values to the original coordinate system, and then figure out the values of each interpolation point in the original coordinate system. The specific algorithm is as follows:

□ First, find the center $P_0(x_0, y_0, z_0)$ and radius r of the arc.

Plane M is determined by three points $P_1(x_1, y_1, z_1)$ 、 $P_2(x_2, y_2, z_2)$ and $P_3(x_3, y_3, z_3)$, and its equation is:

$$\begin{vmatrix} x - x_3 & y - y_3 & z - z_3 \\ x_1 - x_3 & y_1 - y_3 & z_1 - z_3 \\ x_2 - x_3 & y_2 - y_3 & z_2 - z_3 \end{vmatrix} = 0 \tag{9}$$

By expanding the formula, get:

$$\begin{aligned} &[(y_1 - y_3)(z_2 - z_3) - (y_2 - y_3)(z_1 - z_3)](x - x_3) \\ &+[(x_2 - x_3)(z_1 - z_3) - (x_1 - x_3)(z_2 - z_3)](y - y_3) \\ &+[(x_1 - x_3)(y_2 - y_3) - (x_2 - x_3)(y_1 - y_3)](z - z_3) = 0 \end{aligned} \tag{10}$$

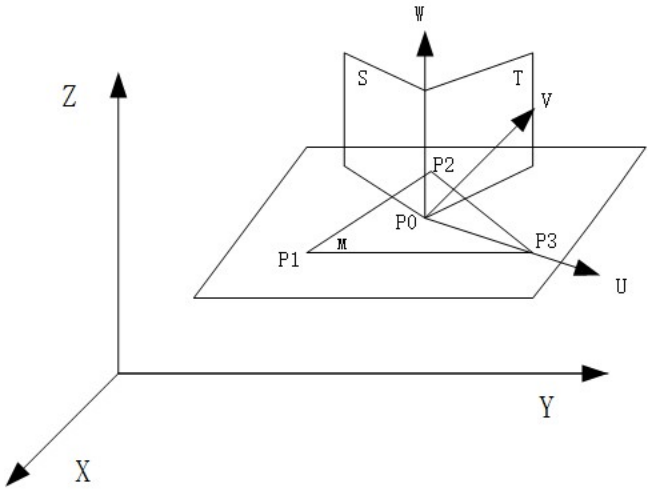

Fig. 4. Spatial circular interpolation diagram

The equation of plane T, which passes through the midpoint of P_1P_2 and is perpendicular to P_1P_2, is:

$$[x - \frac{1}{2}(x_1 + x_2)](x_2 - x_1) + [y - \frac{1}{2}(y_1 + y_2)](y_2 - y_1) + [z - \frac{1}{2}(z_1 + z_2)](z_2 - z_1) = 0 \tag{11}$$

The equation of plane T, which passes through the midpoint of P_2P_3 and is perpendicular to P_2P_3, is:

$$[x-\frac{1}{2}(x_2+x_3)](x_3-x_2)+[y-\frac{1}{2}(y_2+y_3)](y_3-y_2)+[z-\frac{1}{2}(z_2+z_3)](z_3-z_2)=0 \quad \textbf{(12)}$$

If the above equation is combined, the center $P_0(x_0,y_0,z_0)$ is obtained. The radius of the arc is:

$$r=\sqrt{(x_0-x_1)^2+(y_0-y_1)^2+(z_0-z_1)^2} \quad \textbf{(13)}$$

□ The new coordinate O_R-UVW of the plane of the arc is established with the center $P_0(x_0,y_0,z_0)$ as the origin, and the U axis is the line connecting the origin P_0 of the coordinate system with the point P_3. The unit direction vector is $u=\frac{\vec{P}_0\vec{P}_3}{\left|\vec{P}_0\vec{P}_3\right|}$

□ Axis W is the intersection line between plane T and plane S, and its unit direction vector is: $w=\frac{\vec{P}_1\vec{P}_2\times\vec{P}_2\vec{P}_3}{\left|\vec{P}_1\vec{P}_2\times\vec{P}_2\vec{P}_3\right|}$; According to the right-hand rule, the unit vector of the V axis in the cross product direction of the W axis and the U axis is $v=w\times u$

According to homogeneous coordinate transformation, the homogeneous coordinate matrix T_R can be obtained as follows:

$$T_R=\begin{bmatrix} u_x & v_x & w_x & x_o \\ u_y & v_y & w_y & y_o \\ u_z & v_z & w_z & z_o \\ 0 & 0 & 0 & 1 \end{bmatrix} \quad \textbf{(14)}$$

Its inverse matrix T_R^{-1} can be obtained by solving the inverse according to the homogeneous transformation matrix:

$$R=\begin{bmatrix} u_x & v_x & w_x \\ u_y & v_y & w_y \\ u_z & v_z & w_z \end{bmatrix}, P_o=\begin{bmatrix} x_o \\ y_o \\ z_o \end{bmatrix} \quad \textbf{(15)}$$

$$\text{so: } T_R^{-1}=\begin{bmatrix} R^T & -R^TP_o \\ 0 & 1 \end{bmatrix};$$

□ Transform the values of points P_1, P_2, P_3 and center P_o from the original coordinate system to the new coordinate system of center P_0-UVW. Let's say the values in the original coordinate system are (x_1,y_1,z_1), (x_2,y_2,z_2), (x_3,y_3,z_3), (x_o,y_o,z_o).

In the new coordinate, the values are (u_1,v_1,w_1) 、(u_2,v_2,w_2) and (u_3,v_3,w_3), respectively, then the solution is solved.

$$\begin{bmatrix} u_1 \\ v_1 \\ w_1 \\ 1 \end{bmatrix}=T_R^{-1}\begin{bmatrix} x_1 \\ y_1 \\ z_1 \\ 1 \end{bmatrix} \quad \textbf{(16)}$$

$$\begin{bmatrix} u_2 \\ v_2 \\ w_2 \\ 1 \end{bmatrix} = T_R^{-1} \begin{bmatrix} x_2 \\ y_2 \\ z_2 \\ 1 \end{bmatrix} \tag{17}$$

$$\begin{bmatrix} u_3 \\ v_3 \\ w_3 \\ 1 \end{bmatrix} = T_R^{-1} \begin{bmatrix} x_3 \\ y_3 \\ z_3 \\ 1 \end{bmatrix} \tag{18}$$

From the above equation, we can get: $u_o = v_o = w_0 = w_1 = w_2 = w_3 = 0$, $u_1 = r$;

□ Find the arc Angle θ. In MATLAB, the internal function math.atan2 (x, y) has a solution range of -1800-1800. Is:

When $v_3 > 0$, then $\theta_3 = A\tan 2(v_3, u_3)$, $\theta = \lambda\theta_3$, $\begin{cases} v = r \times \sin\theta \\ u = r \times \cos\theta \\ w = 0 \end{cases}$

□ Return the interpolation result to the original coordinate, set the coordinate value of point p as (x, y, z) in the original coordinate system, and then

$$\begin{bmatrix} x \\ y \\ z \\ 1 \end{bmatrix} = T_R \begin{bmatrix} u \\ v \\ w \\ 1 \end{bmatrix} \tag{19}$$

From the above results, the positions of interpolation points on the arc can be obtained. The positions of each interpolation point can be calculated according to the linear function whose displacement curve is a parabola, and the corresponding joint angles of each interpolation point can be obtained through inverse kinematics solutions.

Pose p_1, p_2 and p_3 of three points in space can be expressed by the following formula respectively:

$$T_{p1} = \begin{bmatrix} 0 & 0 & 1 & 360 \\ 0 & 1 & 0 & -60 \\ 1 & 0 & 0 & 400 \\ 0 & 0 & 0 & 1 \end{bmatrix}, \; T_{p2} = \begin{bmatrix} 0 & 0 & 1 & 330 \\ 0 & 1 & 0 & 40 \\ 1 & 0 & 0 & 300 \\ 0 & 0 & 0 & 1 \end{bmatrix}, \; T_{p3} = \begin{bmatrix} 0 & 0 & 1 & 280 \\ 0 & 1 & 0 & 60 \\ 1 & 0 & 0 & 200 \\ 0 & 0 & 0 & 1 \end{bmatrix} \tag{20}$$

4.3 Design and Implementation of Abdominal Needle Assisted Positioning Device

The interpolation steps were set as n = 200, the simulation time was the 40s, and the spatial arc was simulated in V-rep. The degree of freedom of the manipulator should match the task completed. In the M plane, the number of manipulator's joints is redundant for the trajectory of space arcs. The fifth joint axis is consistent with the tool axis at the end. The Angle of joint five does not affect the position and attitude of the tool in the trajectory planning of the space arc.

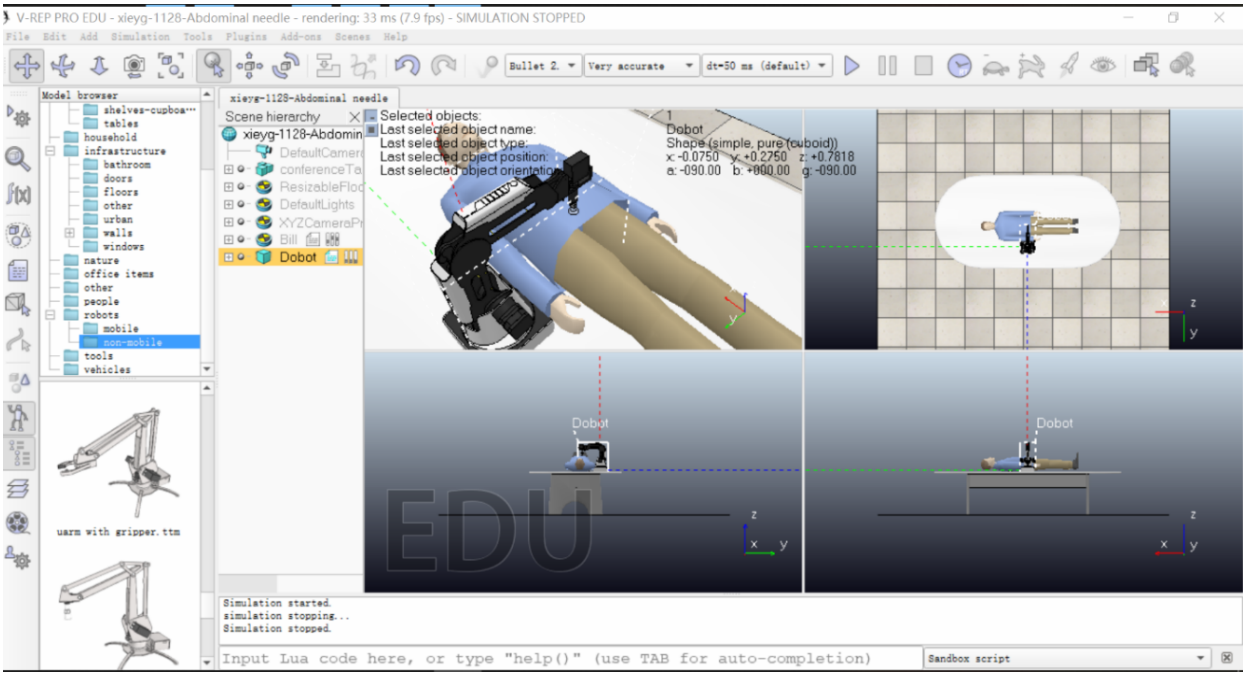

Fig. 5. Spatial circular interpolation diagram

4.4 Motion Control of Abdominal Acupuncture Assisted Acupoint Marking Device

The three signal outputs of the stepper motor are pulse signal PUL, positive and negative control signal DIR and offline signal EN. The principle of stepper motor rotation is that the high and low levels change according to the time interval. The positive and negative control signals of the motor control the direction of motor rotation, and the offline signal of the motor can stop the motor. Firstly, motor positive and negative control signals output high level positive direction rotation. Then set a 4000-step loop and adjust delay to 800ms to vary the high and low levels at the pulse end. In addition, the smaller the time interval, the faster the speed.

5 Abdominal Acupuncture Assisted Acupoint Marking Algorithm

The assisted massage based on abdominal acupuncture points requires lower precision than acupuncture and does not involve acupuncture and moxibustion, which is safer and easier to control. The following acupoint names and international codes are derived from the international recommended standards for acupuncture naming, organized by the western Pacific region office of the world health organization (WHO/WPRO).

The abdomen needle theory divides the human abdomen into three parts, the upper abdomen, the lower abdomen, and the lateral abdomen [2]. See Fig. 6.

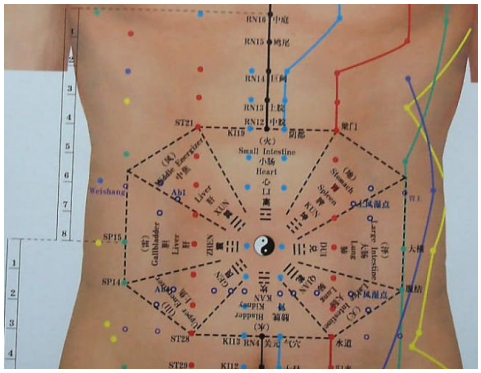

Fig. 6. Abdominal acupoint distribution map

Abdominal needle in the scale positioning will Ren-8 Spirit Palace to the Ren-16 Central Courtyard for 8 units of length [40-41]. The X-axis stepper motor needs to be moved to allow the robot arm to move horizontally to reach the acupuncture point and transfer the step number data of the stepper motor, so as to calculate how many steps each "unit of length" refers to in the function of the stepper motor. After obtaining the data of this unit of length, we can accurately locate the Ren-12 Middle Epigastrium in the location map according to this ratio, 4 units of length on Ren-8 Spirit Palace, 8 units of length on Ren-8 Spirit Palace is the base value just measured. Therefore, we only need to halve the step number of the stepper motor to complete the positioning of Ren-12 Middle Epigastrium. Ren-10 Lower Epigastrium, 2 units of length on Ren-8 Spirit Palace, the same as Ren-12 Middle Epigastrium. The positioning of Ren-12 Middle Epigastrium can be completed by taking the base step number of the motor by 1/4. The following is the detailed design of the acupoint marking algorithm:

(1) lateral ventral reference positioning: the motor of other axes stops, and the motor X is controlled from Ren-8 Spirit Palace (navel) until the digital jump of the lateral waist laser sensor stops immediately.

(2) after the completion of the reference ranging, in order to have a stable starting point for subsequent programs, it is necessary to return the position of the robot arm to zero, that is, to set the port controlling the motor direction to low level, and then repeat the motion cycle function with the base as the parameter.

(3) after completing the datum positioning and returning to zero, the marking of the contralateral abdomen can be formally started, such as St-25 Heaven's Pivot. In Chinese medicine, the definition of this acupoint is to open 2 units of length away from the center of the umbilicus, referring to the previous coordinate system, you can use the reference position parameters, make the X-axis motor to complete 1/3 of the reference cycle, you can position to St-25 Heaven's Pivot. Then the z-axis motor control terminal descends, combined with the laser ranging feedback, just touch the position.

(4) followed by the benchmark: upper abdomen and side abdomen by the same token, the upper abdomen is benchmark Ren-8 Spirit Palace (navel) define the distance to Ren-16 Central Courtyard (chest) for 8 units of length, after the completion of the reference ranging, in order to have a stable starting point for subsequent programs, it is necessary to return the position of the robot arm to zero, that is, to set the port controlling the motor direction to low level, and then repeat the motion cycle function with the base as the parameter.

(5) after completing the datum positioning and returning to zero, the marking of the contralateral abdomen can be formally started, such as Ren-12 Middle Epigastrium. In traditional Chinese medicine, the definition of this acupoint is 4 units of length above the umbilicus. By referring to the previous coordinate system, the reference position parameter can be used to make the Y-axis motor complete 1/2 of the reference cycle in a positive direction, and then the acupoint can be positioned to Ren-12 Middle Epigastrium. Then the z-axis motor control terminal descends, combined with the laser ranging feedback, can reach the position.

The lower abdomen works in the same way as the upper abdomen.

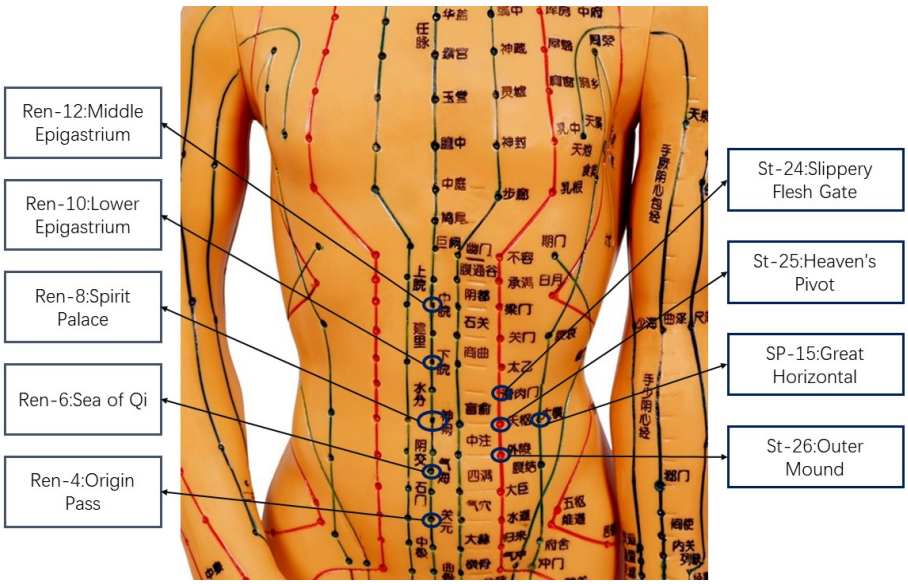

Fig. 7. Schematic diagram of commonly used acupoints for testing

For the abdominal needle-assisted robot completed in this study, the current acupoint positioning accuracy mainly depends on the control accuracy of the stepper motor of each axis of the manipulator, and the fixed-point repetitive positioning error of the manipulator itself is less than 1mm. In the experiment, the abdominal acupuncture doctor conducted an examination after acupoint positioning to judge whether it meets the error requirement of 4mm abdominal acupuncture acupoint massage. Since there is no industry standard for acupoint positioning, the current acupoint error can only be judged subjectively by abdominal acupuncture doctors. For this reason, we conducted 20 tests on commonly used acupoints, and the test error results are shown in Table 1 below.

Table 1. Abdominal acupoint distribution map

Acupoint name	The mean error (mm)	Error minimum (mm)	Maximum error (mm)	Percent of pass (The error is less than 5 mm)
Ren-12: Middle Epigastrium	3.52	2.9	3.9	100%
Ren-10: Lower Epigastrium	3.15	2.8	3.5	100%
Ren-6: Sea of Qi	2.56	2.2	3.1	100%
Ren-4: Origin Pass	3.42	2.9	3.8	100%
St-25: Heaven's Pivot	2.05	1.7	2.4	100%
St-26: Outer Mound	3.14	2.6	3.6	100%
St-24: Slippery Flesh Gate	3.56	2.7	4.1	95%
SP-15: Great Horizontal	3.89	3.3	5.2	70%

It can be seen that the common acupoints around Ren-8 Spirit Palace acupoint are located basically accurately, and the measurement deviation is within 4mm, within the allowable error range of abdominal acupuncture acupoint massage. The main reason is that the acupoint is located in the ventral part, the inclined plane has a large trend, and there is a large vertical drop with Ren-8 Spirit Palace acupoint, which will result in a large positioning deviation of the mechanical arm acupoint. At the same time, since the above positioning process takes Ren-8 Spirit Palace acupoint as the positioning reference point, the experimental process firstly manually adjusts the location of Ren-8 Spirit Palace acupoint, so the accuracy of manual positioning of Ren-8 Spirit Palace acupoint will also affect the experimental results. In addition, since the acupoint results in this experiment were judged by the abdominal acupuncture doctor, artificial errors were also introduced. The total effective rate reached 95.6%.

6 Conclusion

With the development of artificial intelligence technology, medical robots have been widely attention, in the aspect of medical hardware, represented by Leonardo Da Vinci surgical robotic surgical robot, rely on very mature mechanical control and real-time sensing technology, has gained wide acceptance in the clinical and commercial, acupuncture auxiliary robot is one of the important research direction in the current modernization of traditional Chinese medicine, the current research is focused on, such as point diagnosis and automatic positioning technology behind the algorithm, fixed output trajectory with a given trajectory deviation, acupoint location technology based on machine vision, etc.

This project designs and develops a ventral acupuncture assisted mechanical arm that can help doctors to measure and mark acupoints. The single-chip microcomputer control board is used to control the mechanical arm of a large three-axis stepping motor, and the motion planning algorithm of the mechanical arm is used for the coordinated operation of the three-axis motor to realize acupoint marking of ventral acupuncture. This scheme is characterized by effective control of hardware cost, which can meet the functional requirements of an abdominal acupuncture research institute for abdominal acupuncture assistance. The accuracy of auxiliary positioning can meet the requirements of acupoint massage based on abdominal acupuncture, but cannot meet the accuracy requirements of acupuncture. The follow-up work of this topic will be devoted to the automatic identification of Ren-8 Spirit Palace (commonly known as navel), so that the convenience of abdominal acupuncture assisted acupoint marking operation will be greatly increased. At the same time, the machine learning method is improved to improve the accuracy of acupoint location.

Acknowledgements

This work is supported by Beijing Natural Science Foundation (Grant No. 4192023 and 4202024); The Qin Xin Talents Cultivation Program of BISTU. (Grant No. QXTCPC201704); 2018 key research and cultivation projects of BISTU. (5211910953); 2020 key research and cultivation projects information + of BISTU.

References

[1] X.-R. Huang, P.-Y. Zhong, G. Ma, Artificial intelligence and intelligent TCM, Journal of Traditional Chinese Medicine 58(24)(2017) 2076-2079.

[2] H.-L. Zhang, Z.-Y, Bo, Clinical study of “mei nuclear gas” abdominal acupuncture treatment, Capital Food and Medicine 25(20)(2018) 175-176.

[3] H. Wang, P.-Q. Fan, Y.-S. Wang, C. Li, Research on precision control of robot Arm based on ROS platform, Light Industry Machinery 36(6)(2018) 42-47.

[4] X.-L. Wang, L.-X. An, H.-Z, Zhang, Analysis and simulation of robot Arm error based on calibration method of kinematics parameters, Mechanical & Electrical Engineering 2(2019) 109-116.

[5] M. Tan, S. Wang, Research progress in robotics, Acta Automatica Sinica 39(7)(2013) 963-972. DOI:10.3724/SP.J.1004. 2013.00963.

[6] Z. Xie, L. Jin, X. Du, X. Xiao, H. Li, S. Li, On generalized RMP scheme for redundant robot manipulators aided with dynamic neural networks and nonconvex bound constraints, IEEE Transactions on Industrial Informatics 15(9)(2019) 5172-5181. DOI:10.1109/TII.2019.2899909.

[7] J. Dong, B. He, M. Ma, C. Zhang, G. Li, Design of open-closed-loop iterative learning control with variable stiffness for multiple flexible manipulator robot systems, IEEE Access 7(2019) 23163-23168. DOI:10.1109/ACCESS.2019.2898266.

[8] Z. Liu, Z. Zhao, Q. Lin, T.-C. Xu, Study on acupoint selection principle of intelligent acupuncture robot based on graph theory, World traditional Chinese medicine 13(8)(2008) 1992-1996.

[9] T.-C. Xu, X.-J. Wang, D.-D. Lu, M.-Y. Lu, Q. Lin, X.-Q. Zhang, Y. Cheng, Developing trend and key technical analysis of intelligent acupuncture robot, Chinese Journal of Intelligent Science and Technologies 1(3)(2019) 305-310.

[10] G. Li, H. Huang, H. Guo, B. Li, Dynamic modelling and control for a deployable grasping manipulator, IEEE Access 7(2019) 23000-23011. DOI:10.1109/ACCESS.2019.2897689.

[11] K. Ye, Research on manipulator trajectory planning based on intelligent optimization method, Journal of Science and Technology Economics 26(32)(2018) 61.

[12] K. Li, W. Zhang, Y.-J. Chen, Simulation and analysis of on-orbit operation of flexible space manipulator, Space Control Technology and Application 44(5)(2018) 60-69.

[13] W.-H. You, X.-F. Wang, W.-Q. Lu, X.-J. Xu, H. Zhang, Design of trajectory planning interpolation system for industrial manipulators, Mechanical and Electrical Engineering 2(2019) 190-196.

[14] J.-W. Lu, X.-L. Ping, An optimal time-impact trajectory optimization algorithm for manipulators, Mechanical Science and Technology 38(10)(2019) 1548-1554.

[15] X.-J. Wang, T.-C. Xu, X.-Q. Zhang, C.-Y. Song, Q. Lin, Acupuncture point coordinate measurement based on binocular vision, Electronic measurement technology 41(22)(2018) 66-70.

[16] T.-C. Xu, Research and development of digital meridian intelligent acupuncture robot and its application, Chinese Society of Acupuncture and Moxibustion.

[17] Y. Li, Z.-Z. Shao, Z.-D. Zhao, Z.-P. Shi, Y. Guan, Design of deep reinforcement learning reward function for trajectory planning, in: Proc. Computer Engineering and Application, 2019.

[18] M. Ayyildiz, K. Cetinkaya, Comparison of four different heuristic optimization algorithms for the inverse kinematics solution of a real 4-DOF serial robot manipulator, Neural Computing and Applications 27(4)(2016) 825-836.

[19] L. Jiang, Y. Zhou, K. Sun, H. Liu, The obstacle avoidance control of seven-degree-of-freedom redundant mechanical arm, Optics and Precision Engineering 21(7)(2013) 1795-1802.

[20] L. Zhang, N.-F. Xiao, A novel artificial bee colony algorithm for inverse kinematics calculation of 7-DOF serial manipulators, Soft Computing 23(2019) 3269-3277. DOI:10.1007/s00500-017-2975-y.

[21] N. Rokbani, A.-M. Alimi, Inverse kinematics using particle swarm optimization, a statistical analysis, Procedia Engineering 64(2013) 1602-1611.

[22] T.-Y. Fang, H.-C. Zhang, K. Finocchi, Rodolfo, Taylor, H. Russell, Boctor, M. Emad, Force-assisted ultra-sound imaging system through dual force sensing and admittance robot control, International Journal of Computer Assisted Radiology and Surgery 12(6)(2017) 983-991.

[23] Y.-Z. Wang, L. Wei, F. Le, Design of picking robot manipulator based on intelligent AC contactor, Journal of Agricultural Mechanization Research 39(6)(2017) 209-213.

[24] L. Chen, C.-L. Zhang, C.-L. Zhao, R.-F. Hu, A hybrid particle swarm optimization algorithm for inverse kinematics of a 7-DOF robot, Robot. DOI:10.13973/j.cnki.robot.180489.

[25] S. Starke, N. Hendrich, S. Magg, An efficient hybridization of genetic algorithms and particle swarm optimization for inverse kinematics, in: Proc. IEEE International Conference on Robotics and Biomimetics, 2017.

[26] S. Starke S, N. Hendrich, D. Krupke, Evolutionary multi objective inverse kinematics on highly articulated and humanoid robots, in: Proc. IEEE/RSJ International Conference on Intelligent Robots and Systems, 2017.

[27] Z.-F. Cai, D.-P. Huang, Y.-Q. Liu, An inverse kinematics solution using particle swarm optimization by manipulator decoupling, Mechanism and Machine Theory 131(2019) 385-405. DOI:10.1016/j.mechmachtheory.2018.09.022

[28] Z.-Y. Bo, Experience in the classification of abdominal acupuncture therapy for autism, Shanxi Traditional Chinese Medicine 30(4)(2014) 11-12.

[29] Z.-Y. Bo, Retrospect and prospect of abdominal needle for 40 years, in: Proc. The Third International Conference on Abdominal Needles 40th Anniversary Review and Prospects, 2012.

[30] M.-A. Adly, E. Abd, S.-K. Hafiz, Inverse kinematics using single and multi-objective particle swarm optimization, in: Proc. 28th International Conference on Microelectronics, 2016.

[31] F.-J. Yin, Q.-H. Liang, X. Chen, Z.-Y. Tao, Joint space trajectory planning algorithm based on time optimal, Mechanical Design and Research 33(5)(2017) 12-15.

[32] H. Chen, L.-S. Li, Time-optimal manipulator trajectory planning based on compound shape method, Mechanical transmission 43(3)(2019) 72-75+94.

[33] J. Gregory, A. Olivares, E. Staffetti, energy-optimal trajectory planning for robot manipulators with holonomic constraints, Systems & Control Letters 61(2)(2012) 279-291.

[34] J.-H. Lu, X.-L. Ping, An optimal time-impact trajectory optimization algorithm for mechanical arm, Journal of mechanical science and technology 38(10)(2019) 1548-1554.

[35] Y. Yu, M. Lin, Y.-C. Lin, Optimal trajectory planning for industrial robots based on hybrid genetic algorithm, Computer engineering and design 33(4)(2012) 1574-1580.

[36] J. Wu, Research on motion planning of mobile manipulator, [dissertation] Hangzhou, China: Zhejiang University of Science and Technology, 2016.

[37] H.-F. Zhao, Research on the design and control of lightweight and flexible manipulators for human-machine cooperation, [dissertation] Beijing, China: Beijing Jiaotong University, 2017.

[38] X.-X. Liang, Research on key technologies of AC servo control system for industrial manipulators, in: Proc. China Academy of Agricultural Mechanization Sciences, 2017.

[39] K.-R. Xia, Research on virtual decomposition and modal switching control of manipulators for nuclear power disaster relief operations, [dissertation] Harbin, China: Harbin Institute of Technology, 2017.

[40] H.-L. Zhang, Z.-Y. Bo, Clinical study of “Mei nuclear gas” abdominal acupuncture treatment, Capital Food and Medicine 25(20)(2018) 175-176.

[41] Z.-Y. Bo, Experience in the classification of abdominal acupuncture therapy for autism, Shanxi Traditional Chinese Medicine 30(4)(2014) 11-12.